

Converting a Semiconducting Polymer from Ambipolar into n-Type Dominant by Amine End-Capping

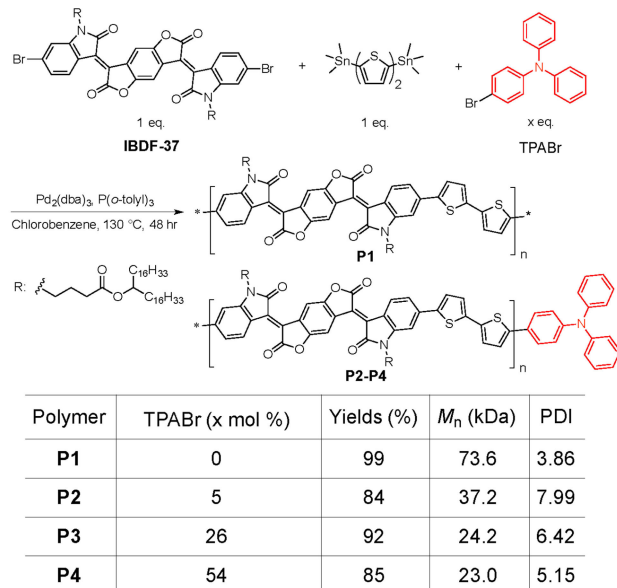
Jesse Quinn,^[a] Haritosh Patel,^[a] Fezza Haider,^[a] Daid A. Khan,^[a] and Yuning Li^{*[a]}

A donor-acceptor polymer of (*3E,7E*)-3,7-bis(2-oxoindolin-3-ylidene)benzo[1,2-*b*:4,5-*b'*]difuran-2,6(3*H*,7*H*)-dione (IBDF) and bithiophene (BT) exhibits typical ambipolar charge transport behaviour in organic thin film transistors. Using the electron rich triphenylamine as an end capping group, a notable suppression of hole transport is observed. This interesting phenomenon is accounted for by the hole trapping effect of the triphenylamine end-capper. Thus, this study provides a novel and facile approach to tuning the charge carrier polarity of a polymer semiconductor from ambipolar to n-type dominant.

Donor-acceptor (D–A) polymers have drawn much attention recently owing to their high charge carrier mobilities in OTFTs^[1–3] and high power conversion efficiencies in OPVs.^[4–6] The push-pull effect of the adjacent donor and acceptor units in this type of polymers results in narrow band gaps and therefore some of them have shown both electron and hole (namely ambipolar) transport performances.^[7–9] This unique ambipolar charge transport characteristic may open up some new applications such as single-component complementary metal oxide semiconductor (CMOS)-like logic circuits^[10] and organic light-emitting transistors (OLETs).^[11] Nevertheless, there are certain limitations such as low on-to-off current ratio (I_{on}/I_{off}),^[12] small noise margins, and large power consumption^[13] for OTFTs using ambipolar polymers. On the other hand, n-type polymer semiconductors^[14–16] are relatively sparse when compared to the large library of high performing p-type polymers.^[17–19] Consequently, efforts have been made lately to unipolarize ambipolar polymer OTFTs into n-type OTFTs. One effective method is to raise the Fermi energy (E_F) of the source electrode to impede hole injection by either using a low work function conductor^[20] or by modifying the surface of the electrode with thiols,^[21] cesium salts,^[22] polyethylenimine (PEI),^[23] or polyfluorene derivatives.^[24] A more facile way is to dope ambipolar polymers with PEI,^[25] aromatic amines,^[26] cesium fluoride,^[27] etc. to raise the E_F of the polymer semiconductors to block hole injection and/or to trap the injected holes.

Our recent study has shown that the hole suppression induced by small aromatic amine dopants to polymer semiconductors is strongly correlated to the trap energy (E_T), which

is defined as the difference between the highest occupied molecular orbital energies (ΔE_{HOMO}) of the dopant and the semiconductor.^[26] It was found that an E_T greater than ~0.3 eV would result in the generation of deep hole traps.^[28] While doping an ambipolar polymer with a small molecule aromatic amine is a convenient way to convert the charge carrier polarity into n-type dominant, it was found that the amine dopant molecules are prone to phase separation and form large clusters upon thermal annealing, leading to recovery of hole transport characteristics.^[26] To overcome this issue, in this study we covalently anchor aromatic amine groups to the polymer chain ends. As a proof of concept, we choose triphenylamine to end-cap a D–A polymer of IBDF and BT (**P1** as shown in Scheme 1), which we previously reported to show an ambipolar



Scheme 1. Synthetic route to **P1–P4**.

charge transport behavior,^[29] based on their suitable frontier energy levels to be discussed as follows.

Triphenylamine (TPA) has an E_{HOMO} of ~−5.4 eV based on the theoretical calculation (Figure S1) and cyclic voltammetry data (Figure S6). Therefore, the E_T of this amine relative to **P1**, which has an E_{HOMO} of −5.7 eV, was estimated to be ~0.3 eV, suggesting that this end-capper may be able to function as a deep hole trap for **P1**. To further scrutinize the suitability of TPA as an end-capper for **P1** for the intended purpose, the ground state structure of the repeat unit of **P1** (**M**) and a terminal unit

[a] J. Quinn, H. Patel, F. Haider, D. A. Khan, Prof. Y. Li

Department of Chemical Engineering and Waterloo Institute for Nanotechnology (WIN), University of Waterloo
200 University Ave West, Waterloo, Ontario, Canada N2L 3G1
E-mail: yuning.li@uwaterloo.ca

Supporting information for this article is available on the WWW under <http://dx.doi.org/10.1002/celc.201600628>

with a TPA (MTPA) (Figure 1) were calculated. It is noticed that the presence of TPA has minimal effects on the electron distribution in the lowest unoccupied molecular orbital (LUMO) wavefunction (mainly localized within the IBDF unit). The LUMO energy (E_{LUMO}) of MTPA (-3.35 eV) is only slightly higher than that of M (-3.40 eV). On the other hand, the HOMO wavefunction of MTPA is dramatically different from that of M. The former is localized to the BT and TPA moieties, while the latter spreads over the M molecule. The E_{HOMO} of MTPA is significantly elevated to -4.94 eV in comparison to M (-5.40 eV). The large ΔE_{HOMO} of 0.46 eV between M and MTPA suggests that the TPA-containing terminal unit may be able to function as an intramolecular deep hole trap. Since TPA has minimal effects on the E_{HOMO} , the electron transport of the TPA end-capped polymer may not be impaired.

P1 without TPA end-capping was synthesized using IBDF-37 and 5,5'-bis-(trimethylstanny)-2,2'-bithiophene as comonomers under a typical Stille coupling polymerization condition with the $\text{Pd}_2(\text{dba})_3/\text{P}(\text{o-tolyl})_3$ catalyst system (Scheme 1). **P2–P4** with TPA end-capping were prepared by introducing different amounts (5, 26, or 54 mol% relative to IBDF-37) of the monofunctional 4-bromotriphenylamine (TPABr) under similar polymerization conditions. The number average molecular weights (M_n) and polydispersity indexes (PDIs) were measured to be 73.6 kg mol^{-1} and 3.86 for **P1**, 37.2 kg mol^{-1} and 7.99 for **P2**, 24.2 kg mol^{-1} and 6.42 for **P3**, and 23.0 kg mol^{-1} and 5.15 for **P4**. The GPC trace for **P1** shows a bimodal distribution (Figure S2), which might be due to the aggregation of polymer chains, a phenomenon observed for other IBDF-based polymers^[29] and diketopyrrolopyrrole-based polymers.^[30,31] For **P2–P4**, multimodal distributions are observed, which can be explained by the introduction of 4-bromotriphenylamine to the polymerization system, since some polymers bearing two TPA end groups would stop growth prematurely, resulting in broader and multimodal distributions. A decreasing trend in the molecular weight from **P1** to **P4** is observed, which is

expected as a result of an increasing amount of the monofunctional TPABr.

^1H NMR spectra of these polymers were measured at 120°C and compared with the ^1H NMR spectrum of TPABr (Figure S3 and Figure S4). Due to the aggregation of polymer chains and the overlapping of the resonance peaks of the TPA end groups with those of the polymer backbone, the amounts of end-capping groups could not be determined. Nonetheless, resonance signals in the region of 6.9–7.5 ppm corresponding to those of protons in TPA were observed (most clearly seen for **P4**). Elemental analysis data for **P2–P4** show a steady increase in the nitrogen content compared to **P1**, which supports the increasing amount of TPA in **P2–P4**.

The UV-Vis-NIR absorption spectra of **P1–P4** were measured in chloroform solutions and as thin films (Figure 2). The wavelength of maximum absorbance (λ_{max}) for all polymers ranged from 842 to 846 nm in solution and from 843 to 849 nm in the solid state. A bathochromic shift in the λ_{max} was observed from solution to solid-state for all polymers, which is due to planarization of the polymer backbone and J-aggregation.^[32] Compared to **P1**, **P2–P4** showed slight hypsochromic shifts in the λ_{max} in the solid state, which is most likely due to the shortened polymer conjugation length.

CV measurements were performed on thin films to estimate the frontier energy levels of the polymers (Figure S5). All polymers exhibited very similar E_{LUMO} of $-3.9 \text{ eV} \sim -4.0 \text{ eV}$ and E_{HOMO} of $\sim -5.7 \text{ eV}$, indicating that TPA end-capping had negligible effects on the energy levels of the polymers. According to the computer simulation results discussed above, the terminal unit, MTPA, would have a much lower E_{HOMO} compared with an internal repeat unit M. However, the amounts of TPA groups in **P2–P4** are probably too small to allow the observation of redox signals of the MTPA units in the CV diagrams.

AFM measurements were performed to examine the morphologies of polymer thin films (Figure 3). **P1** showed worm-like aggregates of a few hundred nm in size, which are

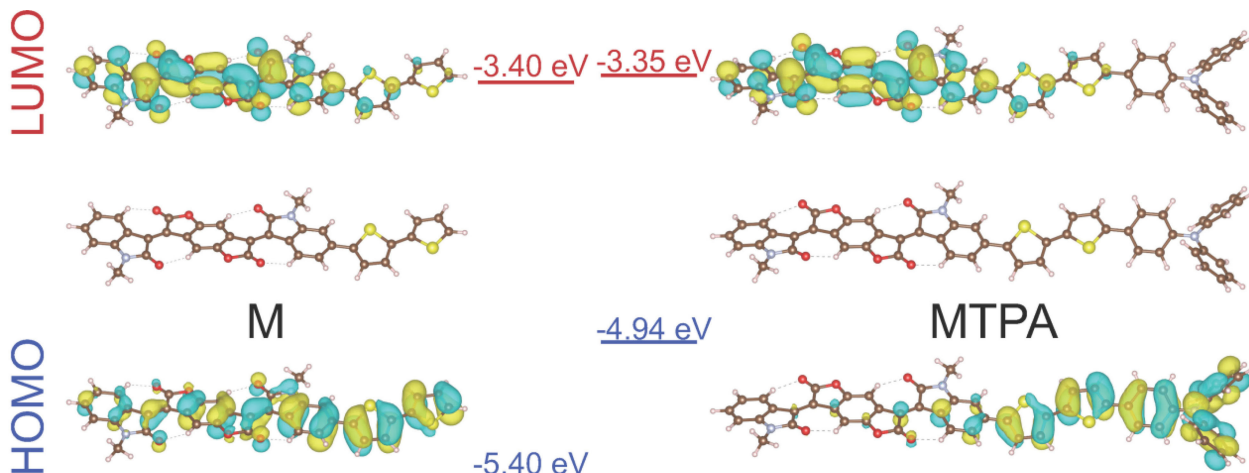


Figure 1. The optimized ground state structures and wavefunctions for the frontier molecular orbitals of the repeat unit of **P1** (M) and the terminal unit with a TPA (MTPA) obtained by DFT calculations at the B3LYP/6-31G(d) level of theory.

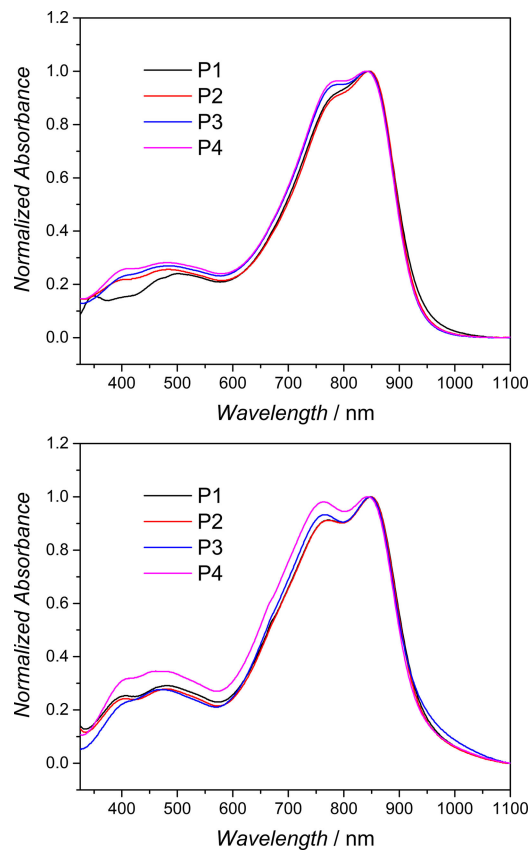


Figure 2. The UV-Vis-NIR absorption spectra of **P1–P4** in chloroform solutions (top) and as thin films (bottom).

composed of small round-shaped grains. All grains and aggregates are tightly joined, forming a very smooth film with a square root roughness (R_q) of ~ 5 nm. The **P2** film has similar round grains and an R_q of ~ 6 nm, but the shape of aggregates of the grains is ill defined compared to **P1**. The morphology of **P3** resembles that of **P1**, but shows larger gaps between the aggregates. The film is much rougher with an R_q of ~ 14 nm. The feature sizes of both the individual grains and aggregates of **P4** become much smaller compared to **P3**, while the film remains quite rough ($R_q = \sim 13$ nm). The observed dramatic changes in the surface morphologies of **P2–P4** compared to **P1** might be linked to the end-capping as well as the decrease in their molecular weight and crystallinity (discussed below).

The X-ray diffraction (XRD) patterns of the spin-coated polymer films exhibited primary diffraction peaks at $2\theta = 3.18^\circ$, 3.17° , 3.10° , and 3.06° , which correspond to *d*-spacings of 2.78, 2.78, 2.85, and 2.88 nm for **P1**, **P2**, **P3**, and **P4**, respectively (Figure S7). It can be seen that as the TPA amount increased, the intensity of the primary diffraction peaks, namely the degree of crystallinity, increased. This trend might be due to the decreasing molecular weight that facilitates the chain packing.^[33]

The charge transport performance of these polymers was evaluated in BGBC OTFT devices. The results are shown in Figure 4, Figure 5, and Table S1. **P1**-based devices showed typical ambipolar charge transport behavior with well-balanced

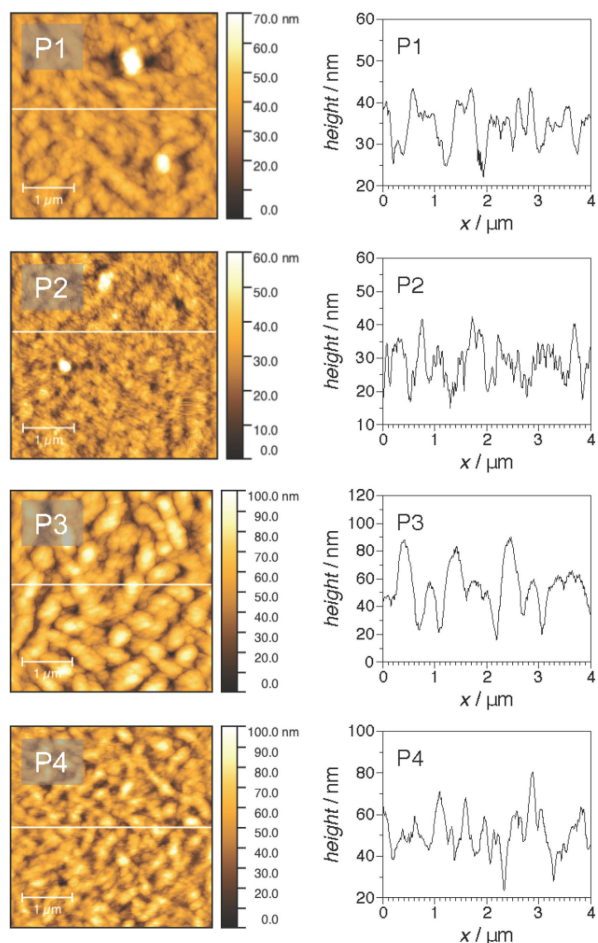


Figure 3. AFM height images ($4 \times 4 \mu\text{m}$) and profiles (scanned along the horizontal lines shown on the respective AFM images on the left) of **P1–P4** thin films annealed at 200°C . The square root roughness (R_q) is 5 nm for **P1**, 6 nm for **P2**, 14 nm for **P3**, and 13 nm for **P4**.

electron and hole mobilities (with an average μ_e/μ_h ratio of 0.96) (Figure 4 and Table S1). The best $\mu_{e,\text{avg}}$ of $2.31 \times 10^{-2} \text{ cm}^2 \text{ V}^{-1} \text{ s}^{-1}$ and $\mu_{h,\text{avg}}$ of $2.24 \times 10^{-2} \text{ cm}^2 \text{ V}^{-1} \text{ s}^{-1}$ were obtained at an annealing temperature of 150°C (Table S1). With a 5 mol% TPABr loading, the resultant **P2** showed a noticeable decline in the hole mobility relative to the electron mobility, increasing the μ_e/μ_h ratio to 1.59. The devices achieved the best $\mu_{e,\text{avg}}$ of $2.72 \times 10^{-2} \text{ cm}^2 \text{ V}^{-1} \text{ s}^{-1}$, and $\mu_{h,\text{avg}}$ of $1.98 \times 10^{-2} \text{ cm}^2 \text{ V}^{-1} \text{ s}^{-1}$ for films annealed at 200°C . By further increasing the TPABr loading to 26 mol%, the resultant **P3** showed a significant reduction in the hole mobility (by $\sim 69\%$) and similar or slightly higher electron mobility values compared to **P1** and **P2**. The μ_e/μ_h ratio is further increased to 4.20. As the TPABr loading is increased to 54 mol% (**P4**), the μ_e/μ_h ratio increased to 25.6 on average, indicating that electron transport has become dominant in the **P4**-based OTFTs (Figure 5). The hole mobility dropped dramatically by $\sim 92\%$, relative to that of **P1**, to an average of $1.6 \times 10^{-3} \text{ cm}^2 \text{ V}^{-1} \text{ s}^{-1}$ for the 200°C -annealed polymer thin films. Interestingly, the average electron mobility increased by nearly two-folds to $4.25 \times 10^{-2} \text{ cm}^2 \text{ V}^{-1} \text{ s}^{-1}$, in comparison to **P1**. The overall increase in the electron mobility from **P1** to **P4** may be attributed to the steady increase in

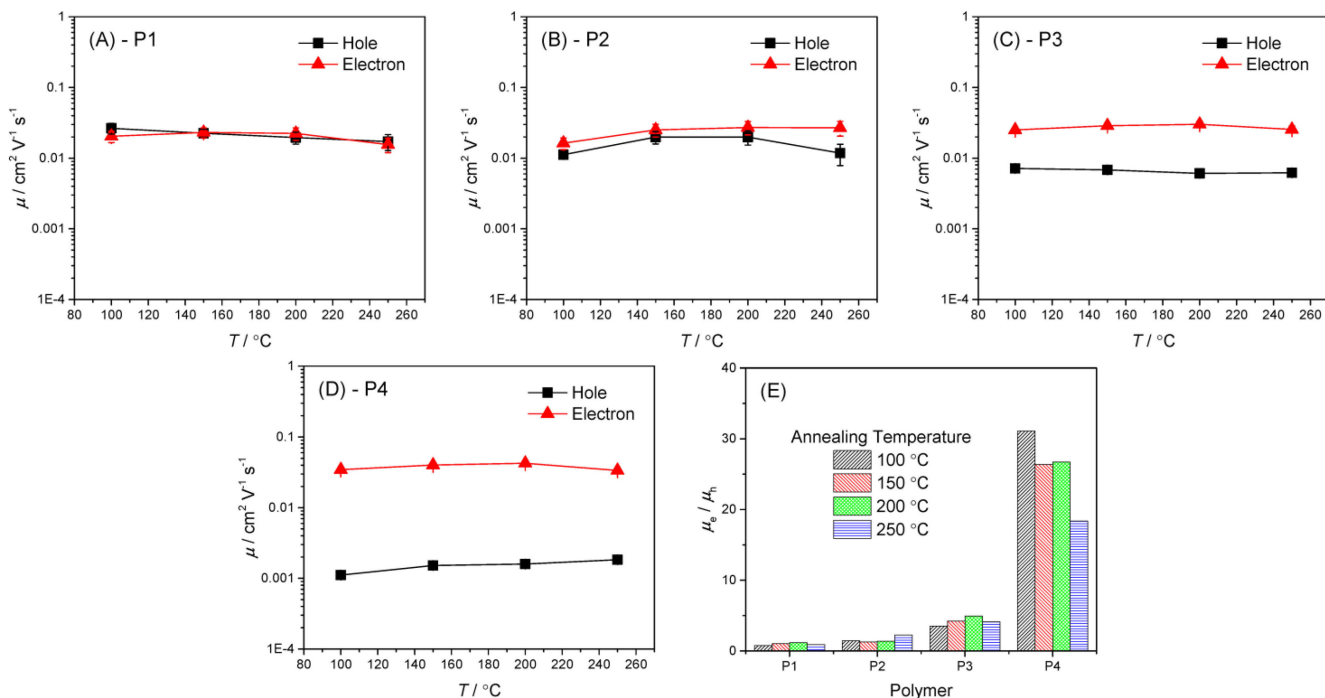


Figure 4. Hole and electron mobilities (A-D) the μ_e/μ_h ratios (E) of OTFT devices based on P1–P4 films annealed at different temperatures..

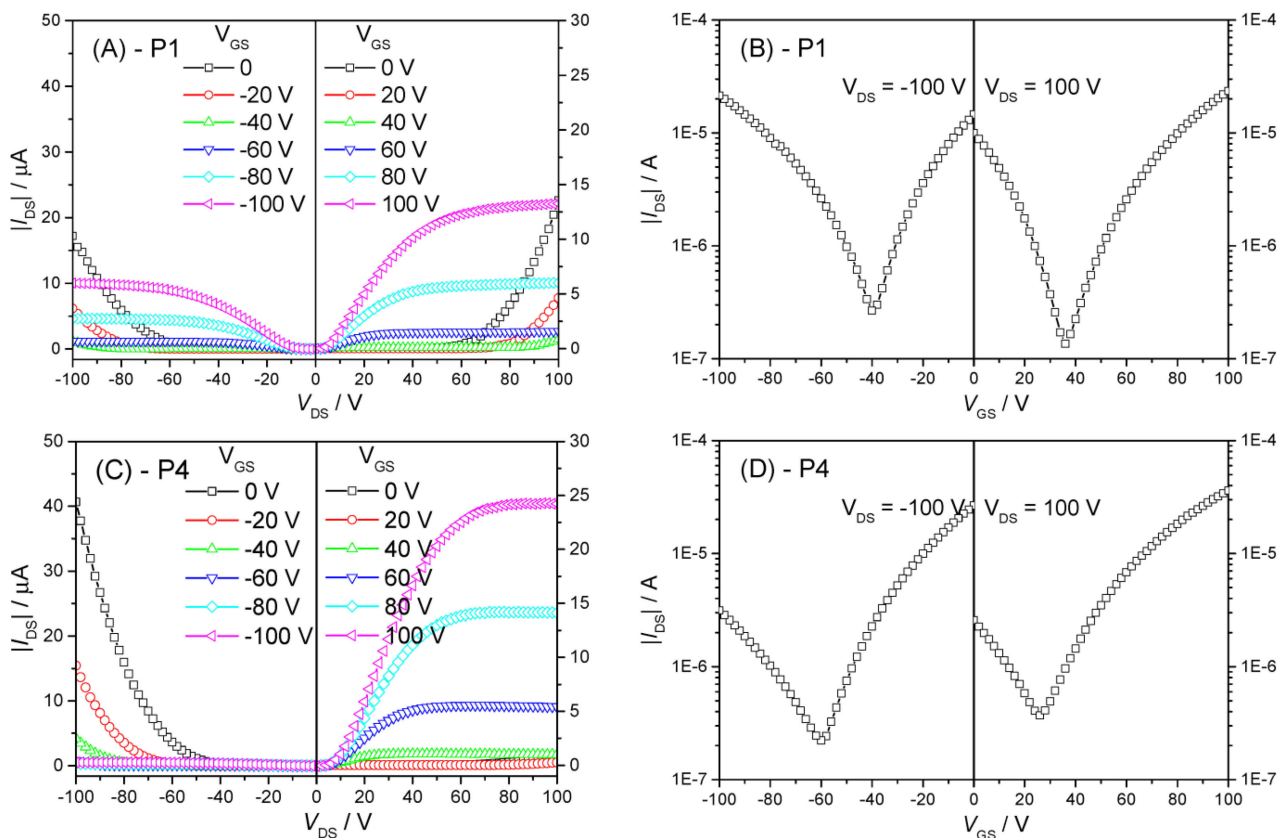


Figure 5. Output (left) and transfer (right) curves of OTFT devices based on P1 (A and B) and P4 (C and D) films annealed at 200 °C.

crystallinity observed by XRD. The reduction in hole transport performance observed for P2–P4 can be accounted for by the

hole trapping effect of the TPA end-capper as discussed above. In addition, the electron rich end-capper may also fill the

electron traps, promoting electron transport.^[34,35] As evidence, the absolute threshold voltage value ($|V_{th}|$), which reflects the charge trap density (hole and electron traps for p-channel and n-channel operations, respectively), increases with increasing end-capper loading of the polymer in the p-channel operation mode (Table S1). In contrast, in the n-channel operation mode, V_{th} showed a decreasing trend with the incorporation of the end-capper, suggesting some electron traps were filled. The TPA end-capped polymer **P4** showed stable n-type electron transport dominant performance at high annealing temperatures up to 200 °C, whereas small molecule amine n-doped polymer systems start to show recovery of hole transport at low annealing temperatures of 80–100 °C due to phase separation.^[26] Therefore, this new end-capping approach is superior in maintaining long term stability of the electron dominant charge transport performance.

In summary, we report a novel method to convert an ambipolar polymer into an electron transport dominant polymer by simply introducing an aromatic amine end-capper. Since the amine end-capper groups are covalently anchored to the polymer chains, the resultant polymers showed robust electron transport dominant performance upon thermal annealing.

Acknowledgements

This work was supported by the NSERC Discovery Grants (RGPIN-2016-04366).

Keywords: ambipolar polymers • n-type polymers • trap energy • triphenylamine • organic thin film transistors

- [1] H.-J. Yun, S.-J. Kang, Y. Xu, S. O. Kim, Y.-H. Kim, Y.-Y. Noh, S.-K. Kwon, *Adv. Mater.* **2014**, *26*, 7300–7307.
- [2] B. Sun, W. Hong, Z. Yan, H. Aziz, Y. Li, *Adv. Mater.* **2014**, *26*, 2636–2642.
- [3] D. Gao, K. Tian, W. Zhang, J. Huang, Z. Chen, Z. Mao, G. Yu, *Polym. Chem.* **2016**, *7*, 4046–4053.
- [4] Y. Zhou, T. Kurosawa, W. Ma, Y. Guo, L. Fang, K. Vandewal, Y. Diau, C. Wang, Q. Yan, J. Reinschach, et al., *Adv. Mater.* **2014**, *26*, 3767–3772.
- [5] Z. Chen, P. Cai, J. Chen, X. Liu, L. Zhang, L. Lan, J. Peng, Y. Ma, Y. Cao, *Adv. Mater.* **2014**, *26*, 2586–2591.
- [6] N. Zhou, A. S. Dudnik, T. I. N. G. Li, E. F. Manley, T. J. Aldrich, P. Guo, H.-C. Liao, Z. Chen, L. X. Chen, R. P. H. Chang, et al., *J. Am. Chem. Soc.* **2016**, *138*, 1240–1251.
- [7] D. Khim, Y. R. Cheon, Y. Xu, W.-T. Park, S.-K. Kwon, Y.-Y. Noh, Y.-H. Kim, *Chem. Mater.* **2016**, *28*, 2287–2294.

- [8] R. Stalder, S. R. Puniredd, M. R. Hansen, U. Koldemir, C. Grand, W. Zajaczkowski, K. Müllen, W. Pisula, J. R. Reynolds, *Chem. Mater.* **2016**, *28*, 1286–1297.
- [9] Y. He, J. Quinn, Y. Deng, Y. Li, *Org. Electron.* **2016**, *35*, 41–46.
- [10] H. Yan, Z. Chen, Y. Zheng, C. Newman, J. R. Quinn, F. Dötz, M. Kastler, A. Facchetti, *Nature* **2009**, *457*, 679–686.
- [11] R. Capelli, S. Toffanin, G. Generali, H. Usta, A. Facchetti, M. Muccini, *Nat. Mater.* **2010**, *9*, 496–503.
- [12] Y. Hu, Q. Lu, H. Li, N. Zhang, X. Liu, *Appl. Phys. Express* **2013**, *6*, 51602.
- [13] H. Klauk, *Chem. Soc. Rev.* **2010**, *39*, 2643.
- [14] H. Li, F. S. Kim, G. Ren, S. A. Jenekhe, *J. Am. Chem. Soc.* **2013**, *135*, 14920–14923.
- [15] M. Nakano, I. Osaka, K. Takimiya, *Macromolecules* **2015**, *48*, 576–584.
- [16] T. Lei, X. Xia, J.-Y. Wang, C.-J. Liu, J. Pei, *J. Am. Chem. Soc.* **2014**, *136*, 2135–2141.
- [17] G. Kim, S.-J. Kang, G. K. Dutta, Y.-K. Han, T. J. Shin, Y.-Y. Noh, C. Yang, *J. Am. Chem. Soc.* **2014**, *136*, 9477–9483.
- [18] J. Y. Back, H. Yu, I. Song, I. Kang, H. Ahn, T. J. Shin, S.-K. Kwon, J. H. Oh, Y.-H. Kim, *Chem. Mater.* **2015**, *27*, 1732–1739.
- [19] Y. Yamashita, F. Hinkel, T. Marszalek, W. Zajaczkowski, W. Pisula, M. Baumgarten, H. Matsui, K. Müllen, J. Takeya, *Chem. Mater.* **2016**, *28*, 420–424.
- [20] G. K. Dutta, A.-R. Han, J. Lee, Y. Kim, J. H. Oh, C. Yang, *Adv. Funct. Mater.* **2013**, *23*, 5317–5325.
- [21] Y. Xu, K.-J. Baeg, W.-T. Park, A. Cho, E.-Y. Choi, Y.-Y. Noh, *ACS Appl. Mater. Interfaces* **2014**, *6*, 14493–14499.
- [22] G. Dell'Erba, A. Luzio, D. Natali, J. Kim, D. Khim, D.-Y. Kim, Y.-Y. Noh, M. Caironi, *Appl. Phys. Lett.* **2014**, *104*, 153303.
- [23] B. Sun, W. Hong, H. Aziz, Y. Li, *Polym. Chem.* **2015**, *6*, 938–945.
- [24] J. Kim, D. Khim, R. Kang, S.-H. Lee, K.-J. Baeg, M. Kang, Y.-Y. Noh, D.-Y. Kim, *Adv. Appl. Mater. Interfaces* **2014**, *6*, 8108–8114.
- [25] B. Sun, W. Hong, E. S. Thibau, H. Aziz, Z.-H. Lu, Y. Li, *ACS Appl. Mater. Interfaces* **2015**, *7*, 18662–18671.
- [26] B. Sun, W. Hong, C. Guo, S. Sutty, H. Aziz, Y. Li, *Org. Electron.* **2016**, *37*, 190–196.
- [27] D. Khim, K.-J. Baeg, M. Caironi, C. Liu, Y. Xu, D.-Y. Kim, Y.-Y. Noh, *Adv. Funct. Mater.* **2014**, *24*, 6252–6261.
- [28] C. Li, L. Duan, H. Li, Y. Qiu, *J. Phys. Chem. C* **2014**, *118*, 10651–10660.
- [29] Y. He, C. Guo, B. Sun, J. Quinn, Y. Li, *Polym. Chem.* **2015**, *6*, 6689–6697.
- [30] Y. Li, P. Sonar, S. P. Singh, M. S. Soh, M. van Meurs, J. Tan, *J. Am. Chem. Soc.* **2011**, *133*, 2198–2204.
- [31] J. R. Matthews, W. Niu, A. Tandia, A. L. Wallace, J. Hu, W.-Y. Lee, G. Giri, S. C. B. Mannsfeld, Y. Xie, S. Cai, et al., *Chem. Mater.* **2013**, *25*, 782–789.
- [32] F. Würthner, T. E. Kaiser, C. R. Saha-Möller, *Angew. Chem. Int. Ed.* **2011**, *50*, 3376–3410.
- [33] R. J. Kline, M. D. McGehee, E. N. Kadnikova, J. Liu, J. M. J. Fréchet, M. F. Toney, *Macromolecules* **2005**, *38*, 3312–3319.
- [34] M. Lu, H. T. Nicolai, G.-J. A. H. Wetzel, P. W. M. Blom, *J. Polym. Sci. Part B Polym. Phys.* **2011**, *49*, 1745–1749.
- [35] Y. Zhang, B. de Boer, P. W. M. Blom, *Phys. Rev. B* **2010**, *81*, 85201.

Manuscript received: October 13, 2016

Accepted Article published: November 10, 2016

Final Article published: December 20, 2016